

MAJOR PAPER

Simultaneous Arterial and Venous Imaging Using 3D Quantitative Parameter Mapping

Tomoki Amemiya^{1*}, Suguru Yokosawa¹, Yo Taniguchi¹, Ryota Sato¹,
Yoshihisa Soutome¹, Hisaaki Ochi¹, and Toru Shirai¹

Purpose: To increase the number of images that can be acquired in MR examinations using quantitative parameters, we developed a method for obtaining arterial and venous images with mapping of proton density (PD), RF inhomogeneity (B1), longitudinal relaxation time (T1), apparent transverse relaxation time (T2*), and magnetic susceptibility through calculation, all with the same spatial resolution.

Methods: The proposed method uses partially RF-spoiled gradient echo sequences to obtain 3D images of a subject with multiple scan parameters. The PD, B1, T1, T2*, and magnetic susceptibility maps are estimated using the quantification method we previously developed. Arterial images are obtained by adding images using optimized weights to emphasize the arteries. A morphology filter is used to obtain venous images from the magnetic susceptibility maps. For evaluation, images obtained from four out of five healthy volunteers were used to optimize the weights used in the arterial-image calculation, and the optimized weights were applied to the images from the fifth volunteer to obtain an arterial image. Arterial images of the five volunteers were calculated using the leave-one-out method, and the contrast between the arterial and background regions defined using the reference time-of-flight (TOF) method was evaluated using the area under the receiver operation characteristic curve (AUC). The contrast between venous and background regions defined by a reference quantitative susceptibility mapping (QSM) method was also evaluated for the venous image.

Results: The AUC to discriminate blood vessels and background using the proposed method was 0.905 for the arterial image and 0.920 for the venous image.

Conclusion: The results indicate that the arterial images and venous images have high signal intensity at the same region as determined from the reference TOF and QSM methods, demonstrating the possibility of acquiring vasculature images with quantitative parameter mapping through calculation in an integrated manner.

Keywords: artery, multi-parameter mapping, relaxation time, susceptibility, vein

Introduction

Various methods have been proposed for the *in vivo* acquisition of quantitative parameter maps related to MR imaging. These maps include longitudinal relaxation time (T1), transverse relaxation time (T2), apparent transverse relaxation

time (T2*), and proton density (PD).¹⁻⁴ A common method, used in techniques such as QRAPMASTER,¹ QALAS,² and DESPOT1/2,³ involves taking multiple images with different scan parameters, such as inversion time (TI) and TE, and fitting them to a function that formulates the relationship between quantitative parameters and the intensity values of the images. In another method, called MR Fingerprinting (MRF),⁴⁻⁶ many images are acquired while changing the scan parameters for each excitation, and quantitative parameters are estimated by matching the obtained signal strength transitions (fingerprint) with simulated signal strength transitions (dictionary). These methods used to obtain relaxation times are called relaxometry. Unlike conventional weighted images, relaxometry enables the quantitative identification of tissues and diseases, which can be expected to improve the accuracy and efficiency of MR

¹Innovative Technology Laboratory, FUJIFILM Healthcare Corporation, Kokubunji, Tokyo, Japan

*Corresponding author: Innovative Technology Laboratory, FUJIFILM Healthcare Corporation, 1-280, Higashi-Koigakubo, Kokubunji, Tokyo 185-8601, Japan. Phone: +81-80-8093-6127, E-mail: tomoki.amemiya.ee@fujifilm.com



This work is licensed under a Creative Commons Attribution-NonCommercial-NoDerivatives International License.

©2022 Japanese Society for Magnetic Resonance in Medicine

Received: December 29, 2021 | Accepted: October 10, 2022

scans.^{1,5–7} For example, it has been suggested that relaxometry by MRF may be able to distinguish low-grade glioma from brain metastasis and glioblastoma.⁷ Weighted images can also be synthesized from the resulting relaxation time maps by means of theoretical formulae¹ or from the scanned images by means of machine learning.^{8,9}

Quantitative susceptibility mapping (QSM) is a method for acquiring quantitative parameters other than relaxation time.^{10–17} Since QSM can perform iron deposition and oxygen extraction fraction measurements,^{12,13} it is expected to be useful for diagnosing cerebral iron deposition in tissues and cerebrovascular diseases. We previously proposed quantitative parameter mapping (QPM) as a method for acquiring T1, T2*, PD, and magnetic susceptibility simultaneously.^{18,19} QPM uses a partially RF-spoiled gradient echo (pRSGE) sequence to obtain images with multiple scan parameters, and by fitting the signal intensity of the images to an intensity function obtained from computer simulation, it can simultaneously estimate the four parameter maps and the RF inhomogeneity (B1).

To extend these parameter-mapping methods, several methods have also been proposed for acquiring arterial images at the same time as the relaxation time and magnetic susceptibility. Conventionally, arterial images are often captured by specific sequences such as the time-of-flight (TOF) method that detects the change in signal intensity caused by the inflow of blood, and they are difficult to directly synthesize from quantitative images obtained by relaxometry. Efforts have been made to address this issue by proposing a method with which scanned images that contain high-intensity images of the blood vessels are combined,²⁰ and a method with which a neural network is used to synthesize scanned images so as to resemble a TOF image.⁹ Even with QPM, it has been shown that arterial images can be obtained by using weighted addition to emphasize arteries.²¹

Venous images can also be obtained from magnetic susceptibility maps by using the difference in magnetic susceptibility.^{12–14} Sequences have also been proposed that can be used to simultaneously obtain an arterial image with the TOF method and a venous image by QSM or susceptibility weighted imaging (SWI).^{22–24}

These arterial and venous images are important for diagnosing cerebrovascular diseases and can be used as markers for identifying the location of lesions in brain surgery,²⁵ providing information that is different from the quantitative parameters obtained from tissue, such as relaxation time and magnetic susceptibility.

As described above, there have been reports of methods for acquiring arterial or venous images without additional scans in the mapping of relaxation time or magnetic susceptibility. However, we have not found any reports in which all of these measurements are done in an integrated manner.

To increase the number of images that can be acquired in MR examinations using quantitative parameters, we propose a method for obtaining arterial and venous images through

calculation, all with the same spatial resolution, in the mapping of PD, B1, T1, T2*, and magnetic susceptibility through calculation. An arterial image is calculated by the weighted addition of images obtained with the parameter-mapping methods with weights predetermined on the basis of datasets of pRSGE images and a reference arterial image. A venous image is calculated from a magnetic susceptibility map by using morphology filtering. We evaluated this method using images of healthy volunteers.

Materials and Methods

Proposed method

Figure 1 shows an overview of the proposed method. Quantitative parameter maps and vascular images are obtained by (1a) capturing 3D images using pRSGE sequences under multiple imaging conditions, (1b) estimating relaxation time, (1c) synthesizing artery images, (1d) estimating magnetic susceptibility maps, and (1e) generating venous images.

In the imaging step (Fig. 1a), scans with a multi-echo pRSGE sequence are performed as in our previous reports,^{18,19} and we used these scans to obtain 17 separate images with different imaging conditions (TR, flip angle [FA], RF phase increment value [θ], and TE, as shown in Table 1). In this study, the combination of these imaging conditions was determined on the basis of the previous reports,^{18,19} and modified to scan the whole brain and blood vessels.

As shown in the same table, in addition to pRSGE, we obtained images with the TOF method used for weight determination and evaluation during arterial-image calculation, and QSM images using RF-spoiled gradient echo for evaluating venous images. Details of the imaging conditions used for our evaluation are described in the Experiments section.

In the relaxation-time-estimation step (Fig. 1b), the T1, T2*, PD, and B1 parameter maps are simultaneously estimated by fitting the intensity function obtained from Bloch simulation to the intensity values of the 17 scanned images.^{18,19} The fitted parameters are restricted to the same range as in the previous report.¹⁹ In the arterial-image-calculation step (Fig. 1c), an arterial image is calculated from the scanned image and the PD, T1 and T2* maps by weighted addition with weights predetermined using the datasets of other subjects. A flowchart of the arterial-image calculation process is shown in Fig. 2. In this method, an arterial image is synthesized by weighted addition of the images of the first echo of each condition (I1, I2, ... I5), which has a high SNR and the maps calculated from these images for each voxel. The weights are determined to increase the contrast between the blood vessel and other tissues in the synthesized arterial image by using a dataset of QPM images and images obtained with the TOF method previously captured from other subjects. A flowchart of the weight-calculation process is shown in Fig. 2 (I). At the normalization step (2a), all scanned images and maps obtained by QPM are normalized so that the

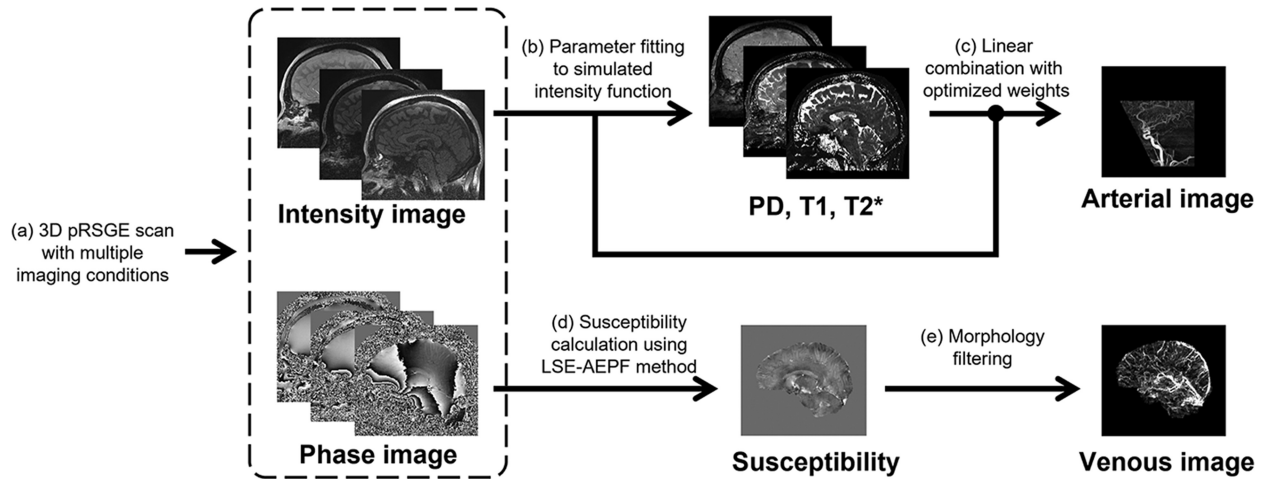


Fig. 1 Processing flow of proposed method. Multiple quantitative parameter maps and vascular images are obtained by (a) capturing 3D images using pRSGE sequences under multiple imaging conditions, (b) estimating relaxation time, (c) synthesizing arterial images, (d) estimating magnetic susceptibility maps, and (e) generating venous images. pRSGE, partially RF-spoiled gradient echo.

Table 1 Scan parameters of the proposed method and comparative methods.

Scan No.	FA (°)	θ (°)	TR (ms)	TE (ms)	Scan time
1	10	20	40	4.6, 11.5, 18.4, 25.3, 32.2	Total: 15 min 56s
2	25	22	20	4.6, 9.2, 13.8	
3	35	2	40	4.6, 11.5, 18.4, 25.3, 32.2	
4	40	5	20	4.6, 9.2, 13.8	
5	40	8	10	4.6	
Ref. TOF	20	117	18	3.4	8 min 40s
Ref. QSM	15	117	46	6.0, 12.0, 18.0, 24.0, 30.0, 36.0	5 min 33s

FA, flip angle; QSM, quantitative susceptibility mapping; TOF, time-of-flight

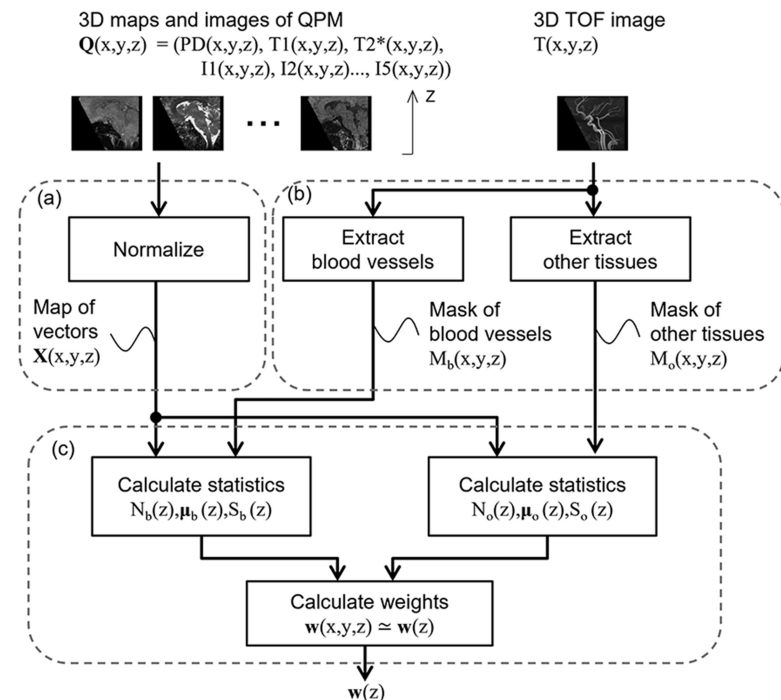
mean and variance become 0 and 1, respectively, resulting in a map X of the vectors of normalized intensity and quantitative parameters. Next, in the region-extraction step (2b), the regions of arteries M_b and other tissues (background tissues) M_o are defined by binarizing the TOF image. The threshold of the binarization was set to 50% of the mean intensity of the manually extracted region in the internal carotid artery. At the weight-calculation step (2c), the number of voxels N , its average value μ , and a variance-covariance matrix S are calculated for the arteries and background tissues at axial slice position Z , and the weights are determined by using linear discriminant analysis (LDA)²⁶ to maximize the between-class variance of arteries and background tissues after the weighted addition. To suppress the variation in weights between adjacent slices, N , μ , and S were calculated including voxels in three slices above and below each. The data of all subjects in the datasets were also included in the calculation. The weights can be determined depending on the 3D position; however, in this study, the weights were determined depending only on Z to simplify calculation.

A flowchart of the arterial-image synthesis process using the calculated weights is shown in Fig. 2 (II). First, we carry out normalization in the same manner as when calculating the weights (2d) and add each slice together after multiplying by the corresponding weight (2e). Since the addition of each axial slice changes the variance of the signal, the output image is normalized again (2f) so that each axial slice in the composite image has a variance of 1.

In the magnetic susceptibility estimation step (Fig. 1d), we used the least squares estimation with adaptive edge preserved filtering (LSE-AEPF)¹⁵ to estimate the magnetic susceptibility from the phase images. The LSE-AEPF method uses multi-echo images in which the conditions other than TE are the same. In this study, we used five multi-echo images of Scan No. 1.

In the venous-image-generation step (Fig. 1e), a venous image is obtained from the magnetic susceptibility map by using a morphology filter bank.²⁷ Multi-scale disk opening operators are applied to the susceptibility map to extract circular components, and the circular components are

(I) Weight calculation



(II) Arterial image calculation

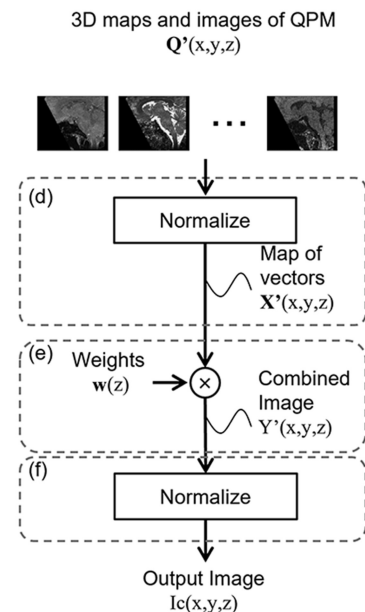


Fig. 2 Weight calculation and image calculation processes used for arterial image generation. (I) Weight calculation using previously captured datasets of QPM and TOF images. (II) Arterial-image calculation from the QPM images. QPM, quantitative parameter mapping; TOF, time-of-flight.

removed to obtain an edge-enhanced susceptibility map as the venous image.

Experiments

This study was approved by the ethics committee of FUJIFILM Healthcare Corporation. All data from healthy volunteers used in this study were obtained after receipt of written informed consent.

To evaluate the proposed method, we performed experiments using five healthy subjects (four males and one female, aged 29–54 years) with a 3-tesla MRI system and a 32-channel head coil (FUJIFILM Healthcare, Tokyo, Japan). Four of these subjects were imaged with the pRSGE and TOF method sequences to optimize the weights used for arterial-image calculation. With the remaining subject, pRSGE and reference TOF methods were also used to evaluate the arterial image synthesized with the proposed method. In addition, a reference QSM method with a conventional RF phase-shift increment of 117° was used to obtain reference venous images for evaluation.

The FOV was $215 \times 215 \times 192$ mm for all sequences, voxel size for the pRSGE and TOF sequences was $0.84 \times 0.84 \times 1.2$ mm, and voxel size for reference QSM was $0.63 \times 0.79 \times 2$ mm. The lower end of the imaging position was set to 3 cm below the foramen magnum.

Other scan parameters of QPM were scan matrix: $256 \times 256 \times 160$ (frequency \times phase \times slice), parallel imaging

factor: 2.0×2.0 (phase \times slice), and slice thickness: 1.2 mm. The total scan time of QPM was 15 min 56s.

Evaluation

To clarify how arterial blood flow affects the signal intensity of scanned images and the calculated quantitative parameters, we first evaluated pixel values in the arteries of four of the subjects for use in weight calculation. Using normalized input images of QPM and arterial mask images obtained by binarizing the TOF images, we calculated the average and standard deviation of the pixel values of the artery regions in each slice, and evaluated the dependence on slice position and variability between subjects.

Next, using the data from these four subjects, we calculated the weights for arterial-image calculation by using the method described in the Proposed method section. The calculated weights were used to synthesize arterial images of the fifth subject (hereafter, test subject) for evaluation.

To calculate and evaluate the arterial image, the number of slices must be the same between subjects. In the reference TOF image, arteries near the top of the head are difficult to extract, so the top 50 axial slices (60 mm) were excluded from calculation and analysis of the arterial image. Artery regions were extracted and arterial images were generated in a range of 95 axial slices (114 mm) containing major arteries, where the intracranial region was extracted by binarization and hole-filling of the scanned images, and the regions

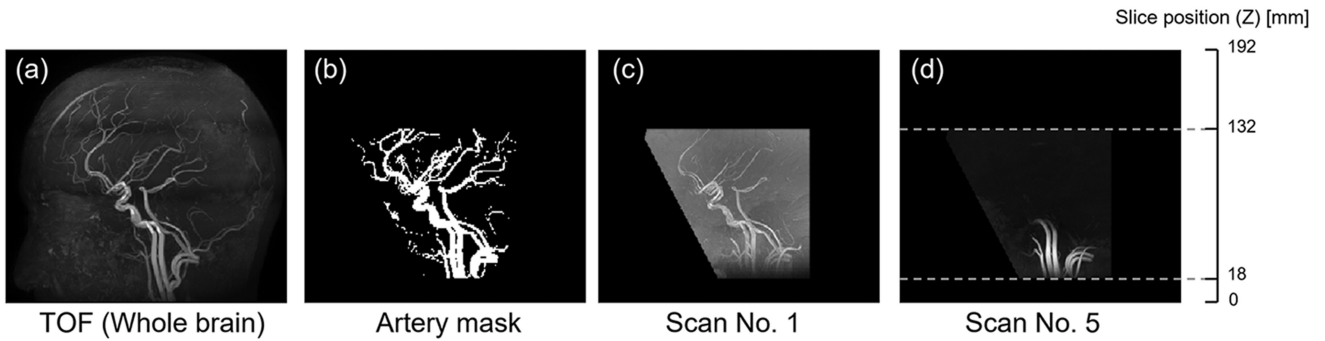


Fig. 3 Example of image used for weight calculation. (a) TOF image, (b) arterial mask image obtained by binarization of TOF image, and (c–d) first echo images of Nos. 1 and 5 QPM scanned images. (MIP to sagittal plane). MIP, maximum intensity projection; QPM, quantitative parameter mapping; TOF, time-of-flight.

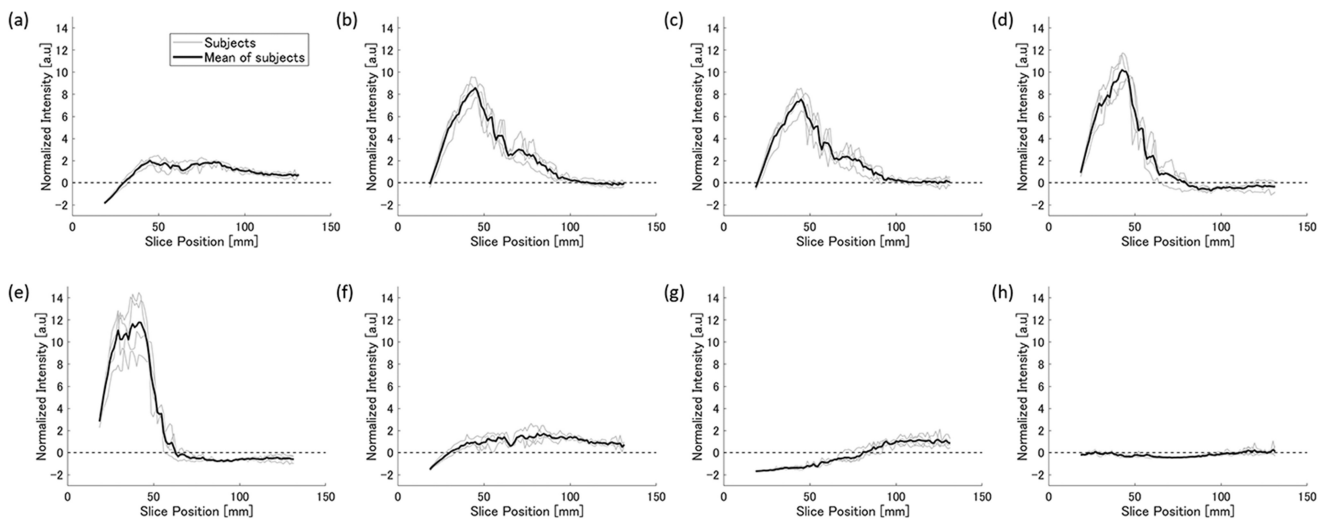


Fig. 4 Average pixel values of arteries in each axial slice of each image and map used in weight calculation. (a–e) First echo images of Scans Nos. 1–5. (f) PD map, (g) T1 map, and (h) T2* map. Pixel values were normalized so that mean and variance through entire region including background tissues would become 0 and 1, respectively. Each line represents individual subject. Thick line represents mean value between subjects. Dashed line represents average value over entire target area (equal to 0 because of normalization). PD, proton density; T1, longitudinal relaxation time; T2*, apparent transverse relaxation time.

corresponding to the eyes and occipital vein sinuses were manually removed.

We then compared the arterial and venous images obtained with the proposed method with images obtained with the reference TOF and QSM methods. Arterial and background regions were defined with the reference TOF image, and the area under the curve (AUC) of the receiver operating characteristic (ROC) curve to discriminate arterial and background was calculated for the intensity of the arterial image obtained by the proposed method. Similarly, the venous and background regions were defined with the reference venous image, and the AUC to discriminate vein and background was calculated for the venous image obtained by the proposed method. The reference QSM and venous images were linearly interpolated to the same resolution as QPM before the comparison.

To evaluate the subject dependency of the arterial-image calculation, the leave-one-out method was applied. By

changing the combination of subjects for weight calculation and the one subject for testing, the arterial image of each of the five subjects was synthesized using weights calculated from the other four subjects. The AUCs for the arterial images were calculated for each subject.

Results

Figure 3 shows (a) a TOF image of one of the subjects used for calculating weights and (b) a mask image of a 3D artery region obtained by binarizing this image. This binarization extracted the artery regions that had high intensity in the TOF image. Also, the first echo images of Scans No. 1 and 5 captured with the proposed method are shown in Fig. 3c and 3d, respectively. Compared with Scan No. 5, Scan No. 1 has higher intensity up to the top of the image (top of the head) but lacks clarity in the lower part of the image

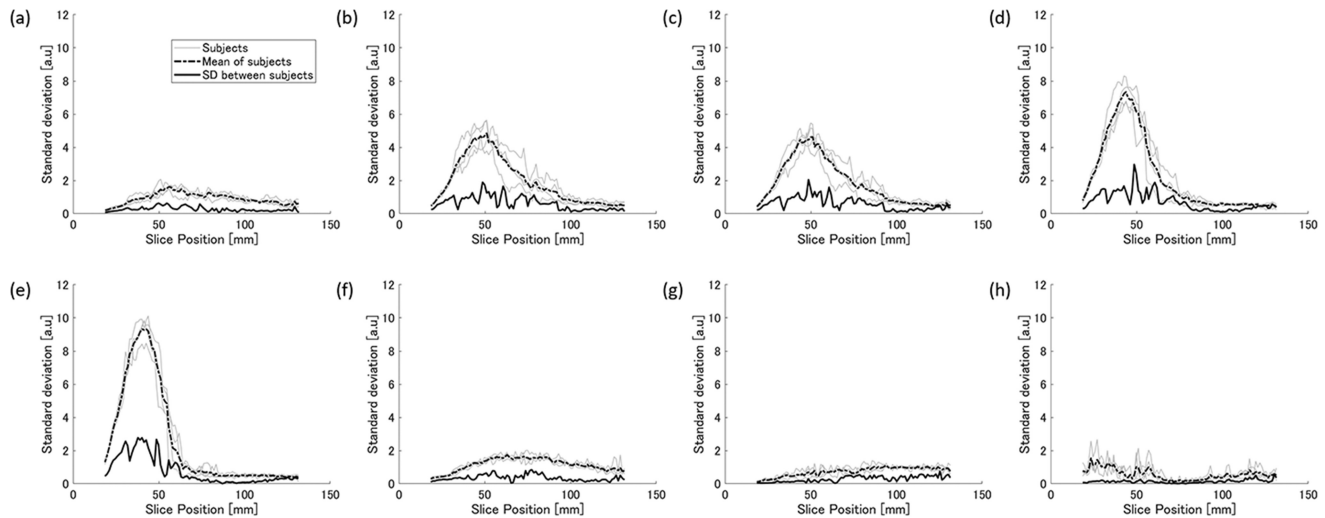


Fig. 5 Standard deviation of artery pixel values in each axial slice of each image and map used for weight calculation. (a–e) First echo images of Scan Nos. 1–5. (f) PD map, (g) T1 map, and (h) T2* map. Each thin line represents standard deviation of individual subject. Dashed line represents average of standard deviations of each subject. Thick line represents standard deviation of average intensity value between subjects. PD, proton density; T1, longitudinal relaxation time; T2*, apparent transverse relaxation time.

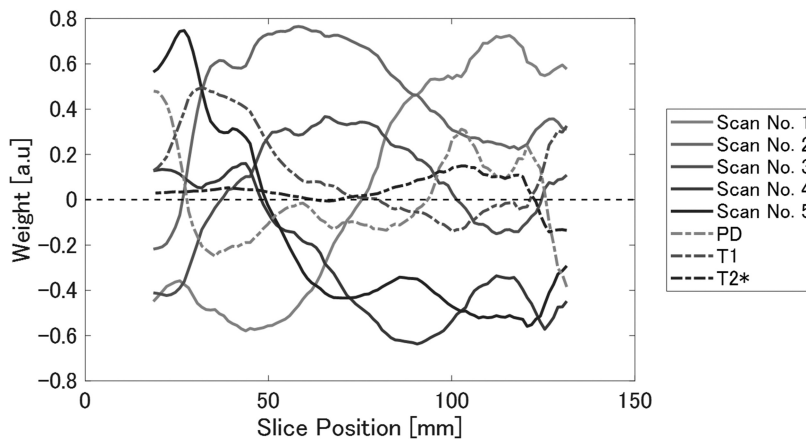


Fig. 6 Weight calculated for each axial slice. Weights differed depending on slice position.

(neck side). In contrast, the neck side in No. 5 is clearly depicted. We thus found that the intensity values of arteries tended to depend on Z .

Figure 4 shows the average pixel value in the artery at each Z in the normalized scanned images (4a–4e) and the quantitative parameter maps (4f–4h) of the four subjects used for the weight calculation. All the scanned images have a peak near 50 mm from the lower end (neck side) of the scanned region and then decrease towards the top of the head, but with different heights and gradients. In particular, Scan No. 1 has a low peak but decreases gradually. However, Scan No. 5 has a high peak and high intensity in the lower part of the image, but the intensity decreases above about 50 mm and falls below the overall average of 0. In addition, the PD image exhibited changes similar to those of Scan No. 1; T1 tended to be shorter (low normalized value) at the lower end of the image and longer toward

the upper end; and T2* was less dependent on slice position than the other parameters. Figure 5 shows the standard deviation for each subject and the standard deviation of the average values between subjects. With the exception of a few slices at the top of the head, the standard deviation between subjects was less than the mean of the standard deviation per subject.

Figure 6 shows the weights for each image calculated using LDA in each slice to emphasize the arteries. On the neck side, the optimized weights are close to 1 in Scan No. 5 and the PD map, but at the top of the head the optimized weights are close to 1 in Scan No. 1 but negative in No. 5. Therefore, the calculated weights differed depending on Z .

Figure 7 shows quantitative parameter maps (PD, T1, T2*, B1, and magnetic susceptibility) of the test subject, an arterial image obtained by weighted addition, and venous image calculated from the magnetic susceptibility. The

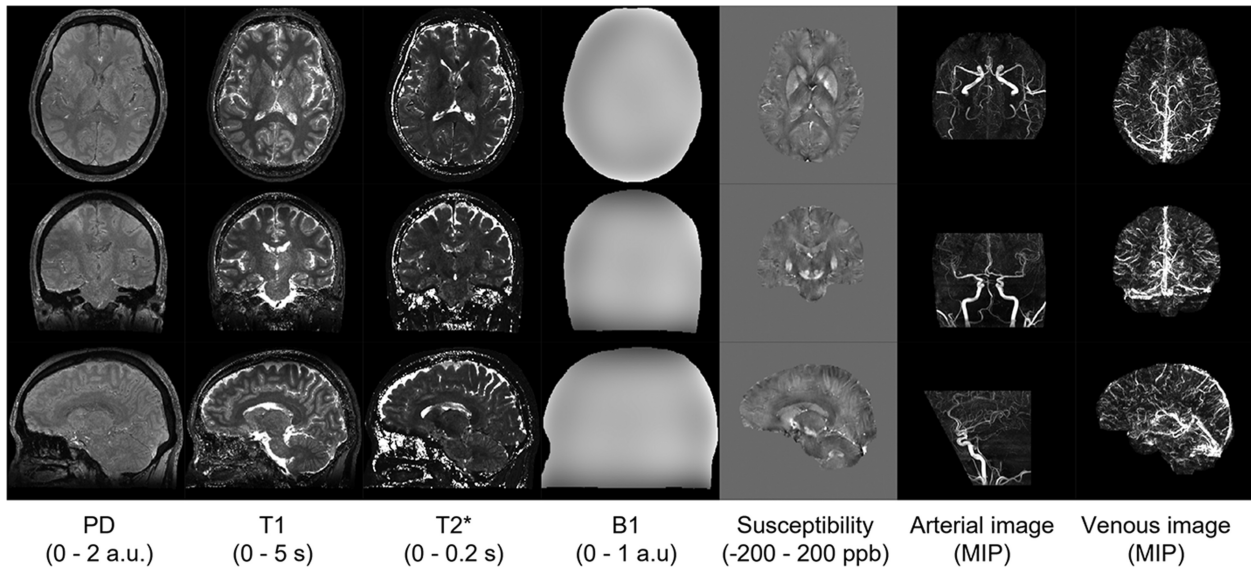


Fig. 7 Quantitative images (axial, coronal, and sagittal slices) and vascular images (MIP to each plane). In each case, artifact-free images were obtained. MIP, maximum intensity projection.

quantitative maps and vascular images were obtained without significant artifacts.

Arterial images of the test subject obtained with the proposed and reference TOF method are shown in Fig. 8a and 8b, respectively. These images were compared using ROC analysis. A histogram of intensity in arterial and background regions with the proposed method is shown in Fig. 8c, and the ROC curve is shown in Fig. 8d. The AUC of the ROC curve was 0.932, and the AUC of the five subjects calculated using the leave-one-out method was 0.905 ± 0.029 (mean \pm standard deviation). The mean of the AUC was significantly higher than 0.5 ($P < 0.01$, t-test).

Venous images of the test subject obtained with the proposed and reference QSM method are shown in Fig. 9a and 9b, respectively. A histogram of intensity in the venous and background regions with the proposed method is shown in Fig. 9c, and the ROC curve is shown in Fig. 9d. The AUC of the ROC curve was 0.920.

Discussion

The results indicate that the proposed method was able to obtain arterial and venous images through calculation from QPM data with weights predetermined using the datasets of other subjects. For arterial images, the proposed method calculates the combination of the intensity images and quantitative maps of QPM with optimized weights for each axial slice. The intensity of the artery regions in the scanned image and the calculated quantitative parameters were position-dependent in the direction perpendicular to the axial slices. This is because the blood flows mainly from the neck to the top of the head, so the change in pixel values due to the inflow effect appears to be large in this direction. The

calculated quantitative parameters are also position-dependent. Normalized values were close to zero at about 50 and 120 mm from the lower end of the imaging position in the PD images and about 80 mm in the T1 images. Normalized T2* values were, compared with PD and T1, close to 0 overall. Therefore, with the widely used methods that calculate a theoretical formula of weighted images to emphasize specific quantitative parameters, there are regions where contrast with the background tissues cannot be achieved. With the proposed method, however, the arteries in their entirety are depicted because the weights of the intensity images and the quantitative map are changed for each axial slice and determined to maximize the contrast between the arteries and background tissue. In other words, the proposed method can retrieve and enhance the relaxation- and flow-properties of arteries that are intrinsically encoded by QPM.

The standard deviation of individual mean normalized values between subjects for each slice was less than the standard deviation for each subject for almost all slices except for a few at the top of the head, suggesting that individual differences in the pattern of pixel value change are small. The leave-one-out evaluation also showed that subject dependency was small so that an arterial image was obtained with the data of a subject different from the subjects for the weight calculation. It is thus considered that the same weights can be used to obtain arterial images from other subjects and error in position settings between subjects are small to avoid the change in the visibility of arteries as long as they are scanned with the same scan position settings and scan parameters.

The venous image from the proposed method also showed high intensity in the same regions as the reference venous image. With the proposed method, veins were extracted by

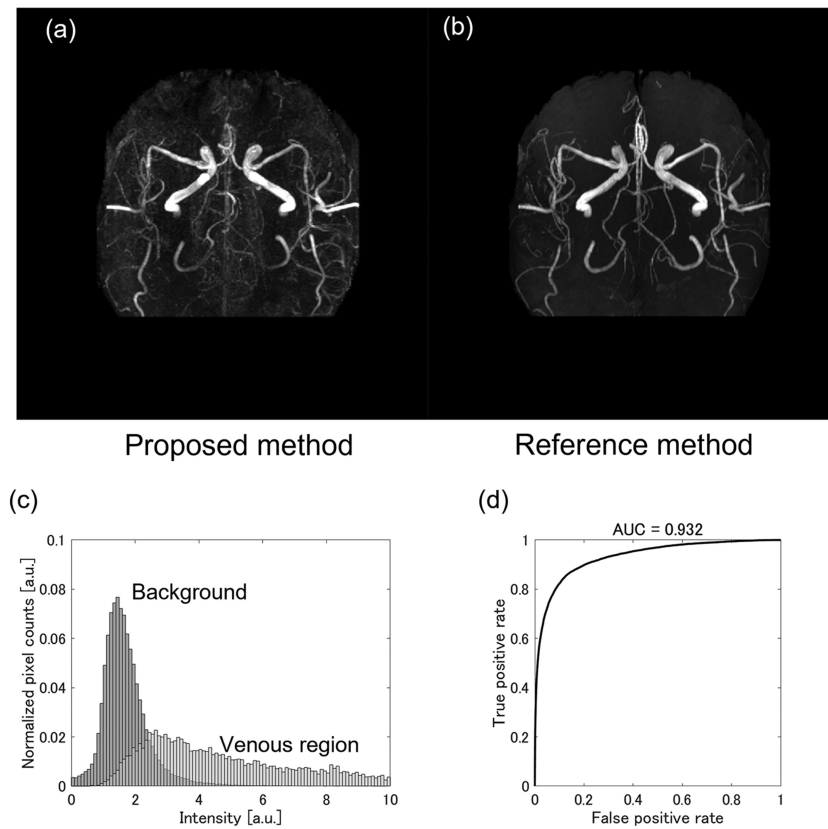


Fig. 8 Comparison of arterial images obtained with proposed method and reference TOF method for test subject. (a) Arterial image from proposed method, (b) reference image from TOF method, and (c) histogram of pixel values of image from proposed method in arterial and background regions defined by reference TOF image. (d) ROC curve of pixel values with proposed method between arterial and background regions. AUC of ROC curve was 0.932. AUC, area under the curve; ROC, receiver operating characteristic; TOF, time-of-flight.

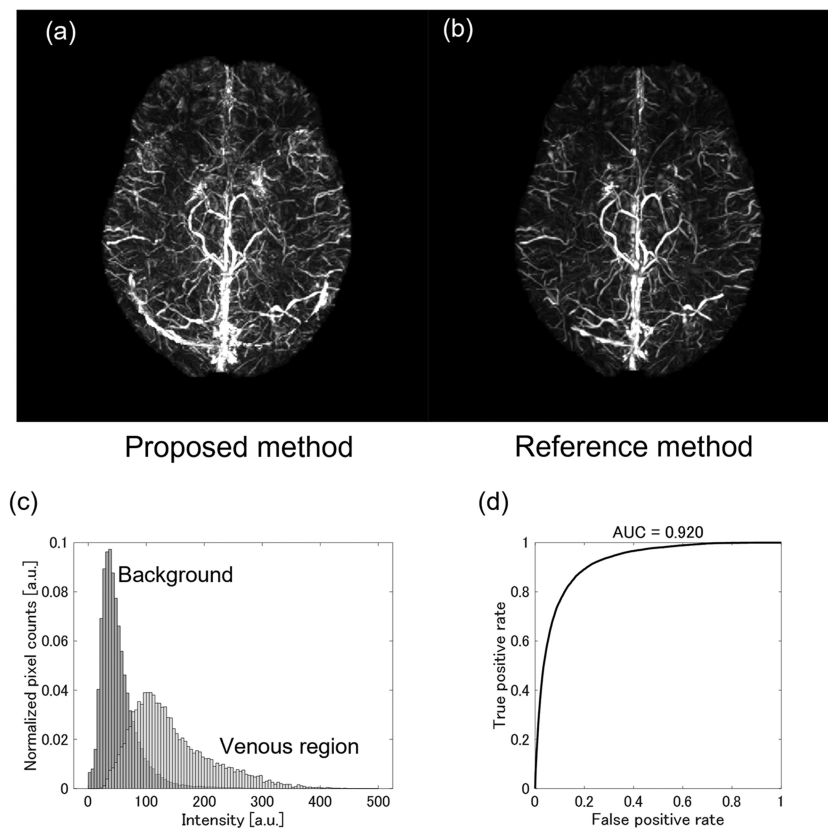


Fig. 9 Comparison of venous images obtained with proposed method and reference QSM method for test subject. (a) Venous image from proposed method, (b) reference venous image, and (c) histogram of pixel values of image with proposed method in venous and background regions defined by reference venous image. (d) ROC curve of pixel values with proposed method between venous and background regions. AUC of ROC curve was 0.920. AUC, area under the curve; QSM, quantitative susceptibility mapping; ROC, receiver operating characteristic.

exploiting the fact that veins have a filamentous structure with higher magnetic susceptibility than their surroundings. A filter is generally used to extract filamentous structures when extracting blood vessels from medical images,^{27,28} and it is thought that veins could be extracted in the same manner by this method.

As described above, our results suggest that the proposed method would enable acquisition of arterial and venous images in addition to relaxation time and magnetic susceptibility measurements. Methods have been proposed for acquiring relaxation time and arterial images simultaneously.^{9,20} Simultaneous acquisition methods for arterial and venous images have also been proposed.^{22–24} However, apart from the present study, we have not found any reports in which all of these measurements are done in an integrated manner. Acquiring these 3D images with the same spatial resolution will make it possible to obtain pre-surgical images of tumors and their surrounding vasculature, which should improve the precision of surgical procedures. For example, veins can be used as landmarks when locating lesions.²⁵ Since various weighted images can be reconstructed from quantitative parameter maps by post-processing, these maps are useful for understanding the morphology of brain tissue. Magnetic susceptibility can also be acquired with this method, enabling the evaluation of bleeding and calcification. In addition, it is expected that differences in relaxation time of tissues can be used to quantitatively indicate the required range of tumor resection. The ability to acquire arterial and venous images in addition to various quantitative parameters in an integrated manner is considered useful for diagnosis and treatment.

Limitations

This study has several limitations. First, the results were obtained from healthy subjects, so the ability of this technique to acquire images of diseased states is unknown. To assess its clinical usefulness, this method will need to be evaluated with a variety of diseases.

Next, the procedure used in this study limits the region to which blood vessels can be visualized. Since arteries at the top of the head were difficult to identify even with the TOF method, we excluded this region from the analysis. In this study, the resolutions in each plane of TOF and QPM were matched at 0.84 mm to facilitate evaluation, but better depiction performance could be achieved by increasing the resolution of the TOF and QPM scans used for weight calculation.

We also manually removed subcutaneous fat, eyeballs, and vein sinuses in advance because their signal intensity differs greatly from that of the intracranial background tissues (principally gray matter, white matter, and cerebrospinal fluid). To make this method more practical, it will need to be developed for automatically segmenting tissues or suppressing these tissues.

The range of venous image generation is also limited. The brain surface was removed when calculating magnetic susceptibility, so it could not be visualized. Methods have been

proposed for calculating magnetic susceptibility with brain surface corrections,^{16,17} and it is thought that these methods will also make it possible to visualize veins on the surface of the brain.

Another limitation is scan time. In this study, parallel imaging was used in the phase and slice direction with a total acceleration factor of 4. However, imaging the entire head with QPM imaging takes about 16 mins, which is not short. The time could be shortened by using other fast imaging techniques such as compressed sensing²⁹ at the same time.

Since there were only four subjects used for calculating weights, we used LDA to avoid the risk of overfitting because LDA has fewer parameters than other discriminant methods, such as deep learning. Subject dependency needs to be further evaluated by increasing the number of subjects. It may also be possible to increase robustness to a wide variety of subjects, such as racial and physical differences, by increasing the number of datasets and calculating the synthesizing function using other methods such as deep learning.⁹ Moreover, larger datasets would suppress variation of the calculated weights or synthesizing function without merging adjacent slices as used in the weight-calculation process in this study.

The weights used in the calculation of an arterial image were supposed to depend on only Z. However, optimal weights would differ in one axial slice. It is possible that calculating weights depending on X and Y in an axial slice in addition to Z, for example based on the dominant area of each artery, will improve the visibility of the arteries.

Conclusion

We proposed a method for acquiring arterial and venous images through calculation in the mapping of PD, B1, T1, T2*, and magnetic susceptibility using pRSGE with multiple imaging conditions. An arterial image is calculated by weighted addition of images obtained in the parameter-mapping method with weights predetermined on the basis of datasets of pRSGE images and a reference arterial image. A venous image is calculated from a magnetic susceptibility map by using morphology filtering. The arterial and venous images from the proposed method had high signal intensity in the same region as the reference TOF and QSM methods. These results indicate the possibility of acquiring arterial and venous images by QPM through calculation in an integrated manner.

Acknowledgments

We thank Professor Kohsuke Kudo (Department of Diagnostic Imaging, Hokkaido University Graduate School of Medicine) for his valuable suggestions in this study.

Conflicts of Interest

All authors are salaried employees of FUJIFILM Healthcare Corporation.

References

- Warntjes JBM, Leinhard OD, West J, Lundberg P. Rapid magnetic resonance quantification on the brain: optimization for clinical usage. *Magn Reson Med* 2008; 60:320–329.
- Kvernby S, Warntjes M, Engvall J, Carlhäll C-J, Ebbens T. Clinical feasibility of 3D-QALAS–single breath-hold 3D myocardial T1-and T2-mapping. *Magn Reson Imaging* 2017; 38:13–20.
- Deoni SCL, Peters TM, Rutt BK. High-resolution T1 and T2 mapping of the brain in a clinically acceptable time with DESPOT1 and DESPOT2. *Magn Reson Med* 2005; 53:237–241.
- Ma D, Gulani V, Seiberlich N, et al. Magnetic resonance fingerprinting. *Nature* 2013; 495:187–192.
- Badve C, Yu A, Rogers M, et al. Simultaneous T1 and T2 brain relaxometry in asymptomatic volunteers using magnetic resonance fingerprinting. *Tomography* 2015; 1:136–144.
- Panda A, Mehta BB, Coppo S, et al. Magnetic resonance fingerprinting – an overview. *Curr Opin Biomed Eng* 2017; 3:56–66.
- Badve C, Yu A, Dastmalchian S, et al. MR fingerprinting of adult brain tumors: initial experience. *AJNR Am J Neuroradiol* 2017; 38:492–499.
- Hagiwara A, Otsuka Y, Hori M, et al. Improving the quality of synthetic FLAIR images with deep learning using a conditional generative adversarial network for pixel-by-pixel image translation. *AJNR Am J Neuroradiol* 2019; 40:224–230.
- Fujita S, Hagiwara A, Otsuka Y, et al. Deep learning approach for generating MRA images from 3D quantitative synthetic MRI without additional scans. *Invest Radiol* 2020; 55:249–256.
- Shmueli K, de Zwart JA, van Gelderen P, Li T-Q, Dodd SJ, Duyn JH. Magnetic susceptibility mapping of brain tissue in vivo using MRI phase data. *Magn Reson Med* 2009; 62:1510–1522.
- Sato R, Shirai T, Taniguchi Y, Murase T, Bito Y, Ochi H. Quantitative susceptibility mapping using the multiple dipole-inversion combination with k-space segmentation method. *Magn Reson Med Sci* 2017; 16:340–350.
- Kudo K, Liu T, Murakami T, et al. Oxygen extraction fraction measurement using quantitative susceptibility mapping: comparison with positron emission tomography. *J Cereb Blood Flow Metab* 2016; 36:1424–1433.
- Haacke EM, Tang J, Neelavalli J, Cheng YCN. Susceptibility mapping as a means to visualize veins and quantify oxygen saturation. *J Magn Reson Imaging* 2010; 32:663–676.
- Xu B, Liu T, Spincemaille P, Prince M, Wang Y. Flow compensated quantitative susceptibility mapping for venous oxygenation imaging. *Magn Reson Med* 2014; 72:438–445.
- Shirai T, Sato R, Taniguchi Y, Murase T, Bito Y, Ochi H. Quantitative susceptibility mapping using adaptive edge-preserving filtering. *Proceedings of the 23rd Annual Meeting of ISMRM, Toronto, 2015; 3319.*
- Shirai T, Sato R, Murase T, Bito Y, Ochi H. Whole brain background field removal using spherical mean value filtering and local polynomial approximation for quantitative susceptibility mapping. *Proceedings of the 26th Annual Meeting of ISMRM, Paris, 2018; 5629.*
- Shirai T, Sato R, Kawata Y, Bito Y, Ochi H. Region Expansion of Background Field Removal with Local Spherical Harmonics Approximation for Whole-brain Quantitative Susceptibility Mapping. *Magn Reson Med Sci* 2022 November 12. [Epub ahead of print]
- Taniguchi Y, Yokosawa S, Shirai T, et al. Fast 3D multi-parameter mapping of relaxation times and susceptibility using partially RF-spoiled gradient echo at 3T. *Proceedings of the 26th Annual Meeting of ISMRM, Paris, 2018; 5630.*
- Taniguchi Y, Yokosawa S, Shirai T, et al. Three-dimensional multi-parameter mapping of relaxation times and susceptibility using partially RF-spoiled gradient echo. *Magn Reson Med Sci* 2022 July 30. [Epub ahead of print]
- Gómez PA, Molina-Romero M, Buonincontri G, Menzel MI, Menze BH. Designing contrasts for rapid, simultaneous parameter quantification and flow visualization with quantitative transient-state imaging. *Sci Rep* 2019; 9:8468.
- Amemiya T, Yokosawa S, Taniguchi Y, et al. Simultaneous acquisition of MR angiography and 3D quantitative MR parameter maps. *Proceedings of the 26th Annual Meeting of ISMRM, Paris, 2018; 2776.*
- Du YP, Jin Z, Hu Y, Tanabe J. Multi-echo acquisition of MR angiography and venography of the brain at 3 Tesla. *J Magn Reson Imaging* 2009; 30:449–454.
- Han M, Burns B, Banerjee S, Lupo J. Multi-band multi-slab 3D multi-echo acquisition for simultaneous time-of-flight MR angiography and susceptibility-weighted imaging at 3T. *Proceedings of the Annual Meeting of ISMRM, 2021; 10.*
- Chen Y, Liu S, Buch S, Hu J, Kang Y, Haacke EM. An interleaved sequence for simultaneous magnetic resonance angiography (MRA), susceptibility weighted imaging (SWI) and quantitative susceptibility mapping (QSM). *Magn Reson Imaging* 2018; 47:1–6.
- Kin T, Nomura S, Shono N, et al. Vascular imaging in surgical simulation for brain tumor. *Jpn J Neurosurg* 2017; 26:480–487.
- Bishop Christopher M. *Pattern recognition and machine learning*. New York:Springer, 2006.
- Hashimoto R, Uchiyama Y, Uchimura K, Koutaki G, Inoue T. Morphology filter bank for extracting nodular and linear patterns in medical images. *Int J Comput Assist Radiol Surg* 2017; 12:617–625.
- Truc PTH, Khan MAU, Lee Y-K, Lee S, Kim T-S, Khan MdAU, et al. Vessel enhancement filter using directional filter bank. *Comput Vis Image Underst* 2009; 113:101–112.
- Lustig M, Donoho D, Pauly JM. Sparse MRI: The application of compressed sensing for rapid MR imaging. *Magn Reson Med* 2007; 58:1182–1195.